



SPE 78483

Fluid Characterisation for Gas Injection Study using Equilibrium Contact Mixing

Koh Takahashi: BUNDUQ Co.Ltd.; Øivind Fevang, PERA, and Curtis H. Whitson: NTNU & PERA

Copyright 2002, Society of Petroleum Engineers Inc.

This paper was prepared for presentation at the 10th Abu Dhabi International Petroleum Exhibition and Conference, Oct. 13-16, 2002.

This paper was selected for presentation by an SPE Program Committee following review of information contained in an abstract submitted by the author(s). Contents of the paper, as presented, have not been reviewed by the Society of Petroleum Engineers and are subject to correction by the author(s). The material, as presented, does not necessarily reflect any position of the Society of Petroleum Engineers, its officers, or members. Papers presented at SPE meetings are subject to publication review by Editorial Committees of the Society of Petroleum Engineers. Electronic reproduction, distribution, or storage of any part of this paper for commercial purposes without the written consent of the Society of Petroleum Engineers is prohibited. Permission to reproduce in print is restricted to an abstract of not more than 300 words; illustrations may not be copied. The abstract must contain conspicuous acknowledgment of where and by whom the paper was presented. Write Librarian, SPE, P.O. Box 833836, Richardson, TX 75083-3836, U.S.A., fax 01-972-952-9435.

Abstract

This paper describes the development of an equation of state (EOS) for a gas injection simulation study of a compositionally-grading near-critical oil reservoir. As the number of initial oil sample was limited and no gas-cap gas compositional data was available, the equilibrium contact mixing (ECM) test was used to (a) help tune the EOS to near-critical phase equilibrium existing at the near-critical gas-oil contact, and (b) to estimate the initial gas-cap PVT properties. Available standard depletion type PVT data, multi-contact swelling test data, slim tube test data and ECM data were used in the development of the full-fluid "detailed" EOS using 16 components. Characterisation of the C_{7+} fraction together with regression of EOS parameters was carried out to tune the fluid model to match all available measured PVT data. Isothermal compositional gradient calculations were performed for all available samples and then a sample was selected to best represent the most important measured properties such as saturation pressure, saturated density and the compositional gradients in the reservoir. Equilibrium contact mixing data provide key gas-cap gas properties and vapour/liquid phase equilibria data for developing the EOS, also important for studying near-miscible gas injection processes.

Introduction

Characterising fluid properties is an essential task for gas injection studies. The composition of initial gas-cap gas is needed to quantify initial condensate in place, and it may impact mixing of injection gas in updip injectors. For near-critical compositionally-grading systems, the estimation of gas-cap gas composition may be important in studying developed miscibility. The gas-cap gas composition may be estimated from compositional gradient calculations from a

down-dip oil sample, however this may lead to considerable uncertainties unless the EOS model has been tuned to near-critical phase data.

In this study we used the equilibrium contact mixing method to obtain equilibrium gas and oil compositions at conditions similar to what are expected at the gas-oil contact. Once tuned to the ECM data, the EOS model is expected to predict more accurately the compositional gradient, gas-oil contact (GOC) location, and gas compositions within the gas cap. This paper provide guidelines for selecting fluid samples and for proper development of an accurate EOS to handle compositional grading calculations and phase behaviour changes in a gas injection project.

Measured Oil and Gas PVT data

There were 20 fluid samples from 13 different wells including 36 constant composition expansion (CCE) tests, 18 differential liberation expansion (DLE) tests, 60 multi-stage separator (SEP) tests, 4 multi-contact swelling (MCV) tests and 3 slintube (SLM) tests.

Since no representative gas cap sample was available, the ECM test¹ was carried out to provide estimates of GOC oil and gas compositions at initial condition, and to determine the richness of the gas-cap gas. This data, when used to tune the EOS model, also provides more certainty that compositional gradients are reliable.

A schematic diagram of the ECM test procedure is shown in Fig. 1. Separator samples were collected from an oil well coning gas-cap gas during testing. The separator samples were then recombined in a proportion which resulted in approximately 50% by volume of equilibrium gas and equilibrium oil at expected initial reservoir conditions near the gas-oil contact. The system was allowed to equilibrate for 24 hours after physical agitation, then the two equilibrium phases were removed separately from the PVT cell for compositional and PVT data measurements.

The resulting equilibrium phases are assumed to provide reasonable estimates of the initial GOC fluids; even if they are not very close to the actual GOC fluids^a, the EOS was tuned to these data so that calculated GOC compositions from an isothermal gradient calculation would be more reliable.

^a The ECM method has less accuracy in predicting actual saturated GOC equilibrium phase compositions when the system is near-critical. This issue is discussed in Ref. 1.

Selection of PVT data for Fluid Characterisation

To determine the validity of available standard PVT samples and laboratory data, plots of saturation pressure versus depth, C_1 mol-% versus depth, C_{7+} mol-% versus depth and C_{7+} molecular weight versus depth were made, as shown in Figs. 2-5. Other cross-plotting methods were used, including a plot of C_{7+} specific gravity versus molecular weight. Data deviating significantly from the trend were not used in the characterisation study, as it is known that a single EOS model will never predict such *outlier* behaviour using a common characterisation.^a

EOS Fluid Characterisation

Splitting the C_{7+} Fraction

The importance of proper characterisation of the heptanes and heavier fractions has been documented previously.^{3,4,5} In this study the C_{7+} fraction was split into five pseudo-fractions using Gaussian quadrature model². The 16-component EOS model generated is shown in Table 1. The Gaussian quadrature model allows multiple reservoir fluid samples from a reservoir to be treated simultaneously with a single fluid characterisation using a special application of the Gamma distribution model³ where

$$z_i = z_{C_{7+}} [W_i f(X_i)] \dots \dots \dots (1)$$

$$M_i = \eta + \beta^* X_i \dots \dots \dots (2)$$

$$f(X_i) = \frac{X_i^{(\alpha-1)} [1 - \ln(\delta)]^\alpha}{\Gamma(\alpha) \delta^{X_i}} \dots \dots \dots (3)$$

where Γ = gamma function and

$$\delta = \exp\left(\frac{\alpha\beta^*}{M_{C_{7+}} - \eta} - 1\right) \dots \dots \dots (4)$$

$$\beta^* = \frac{M_N - \eta}{X_N} \dots \dots \dots (5)$$

The quadrature values of X_i and W_i for $N=5$ are given as follows:

N	X_i	W_i
1	0.263 560 319 718	5.217 556 105 83E-1
2	1.413 403 059 107	3.986 668 110 83E-1
3	3.596 425 771 041	7.594 244 968 17E-2
4	7.085 810 005 859	3.611 758 679 92E-3
5	12.640 800 844 276	2.336 997 238 58E-5

α is the *shape* parameter and η is the minimum molecular weight found in the plus fraction. Gamma model parameters

^a Systematic deviation from a general trend may indicate a separate fluid system requiring a separate EOS model, while random-like deviations from clear trends often are due to experimental data error, or inconsistencies in reported compositional data (compared with the actual samples used in laboratory tests).

were fit using True Boiling Point (TBP) data, with final values of α , η and M_N of 1.7, 90 and 500, respectively. Several individual-feed α values were modified slightly to match the EOS with measured data, especially in MCV results to describe better the critical transition.

Characterising the plus fraction properties

To characterise plus fraction properties, the following equations were used.

Specific gravities. Søreide⁶ correlation:

$$\gamma_i = 0.28554 + C_f (M_i - 65.94)^{0.129969} \dots \dots \dots (6)$$

where $C_f=0.294$ was used to ensure that the measured C_{7+} specific gravities were honoured as accurately as possible.

Normal boiling points. Søreide correlation:

$$T_{bi} = A_1 + A_2 M_i^{-0.03522} \gamma_i^{3.266} \exp[A_3 M_i + A_4 \gamma_i + A_5 M_i \gamma_i] \dots \dots \dots (7)$$

$$A_1 = 1928.3, A_2 = -1.695E-5, A_3 = -4.922E-3 \\ A_4 = -4.7685, A_5 = 3.462E+3$$

Critical properties. Twu⁷ correlations:

Critical temperature of normal paraffins

$$T_{cPi} = T_{bi} \left[A_1 + A_2 T_{bi} + A_3 T_{bi}^2 + A_4 T_{bi}^3 + \frac{A_5}{(A_6 T_{bi})^{13}} \right] \dots \dots \dots (8)$$

$$A_1 = 0.533272, A_2 = 0.191017E-3, A_3 = 0.779681E-7 \\ A_4 = -0.284376E-10, A_5 = 0.959468E+2, A_6 = 0.01$$

Critical pressure of normal paraffins

$$p_{cPi} = (A_1 + A_2 \alpha_i^{0.5} + A_3 \alpha_i + A_4 \alpha_i^2 + A_5 \alpha_i^4)^2 \dots \dots \dots (9)$$

$$A_1 = 3.83354, A_2 = 1.19629, A_3 = 34.8888 \\ A_4 = 36.1952, A_5 = 104.193$$

Specific gravity of normal paraffins

$$\gamma_{pi} = A_1 + A_2 \alpha_i + A_3 \alpha_i^3 + A_4 \alpha_i^{12} \dots \dots \dots (10)$$

$$A_1 = 0.843593, A_2 = -0.128624, A_3 = -3.36159, A_4 = -13749.5$$

where

$$\alpha_i = 1 - \frac{T_{bi}}{T_{cPi}}$$

Critical temperature

$$T_{ci} = T_{cPi} \left(\frac{1 + 2f_{Ti}}{1 - 2f_{Ti}} \right)^2 \dots \dots \dots (11)$$

$$f_{Ti} = \Delta \gamma_{Ti} \left[\frac{A_1}{T_{bi}^{0.5}} + \left(A_2 + \frac{A_3}{T_{bi}^{0.5}} \right) \Delta \gamma_{Ti} \right] \dots \dots \dots (12)$$

$$A_1 = -0.362456, A_2 = 0.0398285, A_3 = -0.948125$$

$$\Delta\gamma_{Ti} = \exp[5(\gamma_{pi} - \gamma_i)] - 1 \dots\dots\dots (13)$$

Critical Pressure

$$p_{ci} = p_{cpi} \left(\frac{T_{ci}}{T_{cpi}} \right) \left(\frac{v_{cpi}}{v_{ci}} \right) \left(\frac{1+2f_{pi}}{1-2f_{pi}} \right)^2 \dots\dots\dots (14)$$

$$f_{pi} = \Delta\gamma_{pi} \left[\left(A_1 + \frac{A_2}{T_{bi}^{0.5}} + A_3 T_{bi} \right) + \left(A_4 + \frac{A_5}{T_{bi}^{0.5}} + A_6 T_{bi} \right) \Delta\gamma_{pi} \right] \dots\dots (15)$$

$$A_1 = 2.53262, A_2 = -46.1955, A_3 = -0.00127885$$

$$A_4 = -11.4277, A_5 = 252.14, A_6 = 0.00230535$$

$$\Delta\gamma_{pi} = \exp[0.5(\gamma_{pi} - \gamma_i)] - 1 \dots\dots\dots (16)$$

Acentric Factor

The acentric factor ω is determined such that the specified normal boiling point for each C_{7+} fraction is matched exactly. If any property (T_c , p_c , or T_b) of a C_{7+} fraction is modified during regression, ω of that fraction is automatically adjusted to guarantee the EOS predicts this equilibrium condition (vapour pressure $p_v=1$ atm at T_b) exactly.

Binary Interaction Parameters C_1 — C_{7+}

Modified Chueh-Parausnitz¹⁰

$$k_{ij} = 0.18 \left[1 - \left(\frac{2v_{ci}^{1/6} v_{cj}^{1/6}}{v_{ci}^{1/3} + v_{cj}^{1/3}} \right)^6 \right] \dots\dots\dots (17)$$

$$v_{ci} \approx 0.4804 + 0.0601 M_i + 0.00001076 M_i^2 \dots\dots\dots (18)$$

The constant 0.18 was determined by regression to improve the saturation pressure predictions.

Parachor

Firoozabadi *et al.*¹¹

$$P_i = 11.4 + 3.23 M_i - 0.0022 M_i^2 \dots\dots\dots (19)$$

C_{7+} Volume Translation Parameters

The volume translation parameters^{12, 13} of the plus fraction were calculated by solving the Peng-Robinson EOS¹⁴.

Molar volume at standard condition is described as

$$v_{sci} = \frac{M_i}{62.37 \gamma_i} \dots\dots\dots (20)$$

Molar volume by 2 parameter P-R EOS

$$p = \frac{RT}{v-b} - \frac{a}{v(v+b)+b(v-b)} \dots\dots\dots (21)$$

The EOS can be expressed as

$$v^3 + A_1 v^2 + A_2 v + A_3 = 0 \dots\dots\dots (22)$$

where

$$A_1 = \frac{pb - RT}{p}$$

$$A_2 = \frac{-3pb^2 - 2RTb + a}{p}$$

$$A_3 = \frac{pb^3 + RTb^2 - ab}{p}$$

by solving Eq.22 under standard condition, each component $v_{EOS-SCi}$ can be calculated.

Volume translation parameter can be calculated as

$$s_i = \frac{c_i}{b_i} \dots\dots\dots (23)$$

$$c_i = v_{EOS-SCi} - v_{SCi} \dots\dots\dots (24)$$

The initial EOS parameters of 16 components are shown in Table 1.

Regression

To match the EOS with measured PVT and compositional data, some modification of the EOS parameters is usually necessary. It is important to use an EOS which can predict vapour/liquid phase behaviour accurately, especially for gas injection process. To develop an EOS which can be used for this gas injection study, we paid particular attention to the measured data of several specially-designed swelling tests using different injection gases, as well as ECM data (most of these data from five different wells).

Several combinations of regression parameters were tried which resulted in a good description of the measured data included in the regression. A total of ten regression parameters were used to obtain an acceptable match of measured PVT data. Also, slight changes in M_{7+} values for (about 20) individual samples were used^a to allow near-exact saturation pressure predictions for all samples. Accurate saturation pressures were important to the compositional gradient calculations.

Viscosities were matched by changing critical volumes of C_{7+} fractions used in LBC¹⁵ viscosity correlation.

^a The reported lab mass fractions were always honoured exactly. When a C_{7+} molecular weight was modified for a specific sample (usually by only a few percent), the conversion from mass to mole fractions resulted in a new molar composition used in EOS calculations.

Final tuned EOS and LBC component properties are shown in Table 2. Results of the data fit are shown in Figs. 6–10. ECM gas and oil composition matching results are shown in Table 3 and 4, and Fig. 11 and 12, respectively.

The measured and calculated saturation pressures for CCE and DLE experiments resulted in about 0.5% difference of the measured data as shown in Fig. 13. The calculated oil volume shrinkage from DLE experiments (B_{od}/B_{odb}) was within 3% of the measured data as shown in Fig. 14. The calculated gas released from solution in the DLE experiments was usually estimated within 5%, and a few samples with up to 10% difference from the measured data, as shown in Fig. 15. The calculated reservoir oil density at the bubble point was within 2–3% for most samples, as shown in Fig. 16.

Reducing Number of Components (*Pseudoization*)

Pseudoization¹⁶ from 16 to 9 component EOS was conducted to minimise the CPU time and memory requirements for full-field simulations.

The approach to reducing the number of components was to generate a wide range of PVT “data” using the final 16-component EOS model for many of the samples. These data included depletion experiments (CCE and DLE), separator tests, complex critical-transition swelling tests and MMP (minimum miscibility pressure) data with several injection gases.

The EOS16 “data” were then used for regression in a stepwise pseudoization procedure. For one step in the process, several components are grouped together. The properties of the newly-formed pseudocomponents are modified to maintain an optimal fit of the EOS16 data. This usually involves modifying the EOS a and b constants and sometimes volume shift factors of the newly-formed pseudocomponents, as well as BIPs of the methane- C_{7+} fractions.

Eventually at some step in the pseudoization process we found that the resulting EOS did not describe key data from the EOS16 data set. After trying all logical groupings without finding a better reduced EOS model, the process was terminated. In this study we ended up with a final 9-component EOS model as shown in Table 5.

Compositional Gradient Calculations

Isothermal compositional gradient predictions were performed individually for all samples using the detailed and pseudoized EOS models.

After analysing the trends in each sample’s compositional gradient, comparing it with measured sample trends in saturation pressure, GOR, and individual component variations (H_2S , C_1 , and C_{7+}), we finally selected one particular sample which seemed to best represent the most important property-depth variations. Based on this particular sample gradient, the GOC was predicted as shown in Fig. 17. The final EOS model after regression of ECM and swelling-test data resulted in a somewhat deeper GOC than the initial model fit to standard depletion PVT data only.

Compositions of the gas-cap gas at predicted GOCs using the final tuned EOS and the old EOS without ECM data were

compared. It was found that the final EOS including ECM data is richer than that the untuned EOS (without ECM data), as shown in Table 6 and Fig. 18.

The gas-cap gas, GOC location, and variations in compositions in the gas cap can impact the gas injection project which relies on injecting lean separator gas into the gas cap, this gas displacing the in-situ gas-cap gas, and finally the in-situ gas-cap gas displacing the initial oil. Because of high permeabilities, the gas displacement has a strong and positive effect of gravity, thereby making the initial gas-cap description particularly important. Without the ECM-type data to help tune the EOS model, a greater uncertainty in the gas injection project would have existed.

Conclusions

1. All representative PVT samples were used in developing an EOS model to be used for (a) fluid initialisation, including gas-oil contact prediction, and (b) miscible gas displacement. More than a thousand PVT data were used, derived from more than 10 samples from a fluid column showing significant compositional grading.
2. Equilibrium-contact-mixing and swelling tests provided important vapour/liquid equilibria data which were important for developing an accurate EOS for estimating initial fluids in place (compositional gradients), gas-cap properties, and studying gas-injection processes.
3. Heptanes-plus characterisation included the use of the Gaussian quadrature model to handle multiple samples with differing C_{7+} bulk properties, and published correlations for initial estimates of C_{7+} component properties. Some C_{7+} component-property modifications were necessary to provide a satisfactory description of all key measured PVT data.
4. Slight modifications from the measured molar distribution was necessary for some samples to help model critical (bubblepoint-to-dewpoint) transitions in the swelling tests.

Nomenclature

a = EOS constant

A_i = numerical constants used in equations

b = EOS constant

c = EOS volume-translation constant

k_{ij} = EOS binary-interaction parameter

K_w = Watson characterisation factor, $^{\circ}R^{1/3}$

M_i = molecular weight, lbm/lbm mole

M_{c7+} = molecular weight of the heptane plus fraction, lbm/lbm

M_N = molecular weight of heaviest heptane plus fraction

p_{cP} = critical pressure of paraffin hydrocarbons, psia

P = parachor

R = universal gas constant = 10.73146 psia-ft³/degR-lbm-mol

s_i = dimensionless volume-translation variables used in EOS

T_b = normal boiling point at 1 atm, degree R

T_{br} = reduced normal boiling point

T_c = critical temperature, degree R

T_{cP} = critical temperature of paraffin hydrocarbons, degree R

v_{cP} = critical volume of paraffin hydrocarbons, ft³/lbm mol

W_i = Gaussian quadrature weight factor
 X_i = Gaussian quadrature point
 Z_i = mole fraction in total system
 Z_{C7+} = mole fraction of the heptane plus fraction
 α = gamma distribution shape parameter,
 Twu property correlation parameter
 β^* = parameter in the modified gamma distribution model
 used with Gaussian quadrature
 γ = specific gravity, air=1
 γ_{cp} = specific gravity of paraffin hydrocarbons, air=1
 δ = parameter in the modified gamma distribution model used
 with Gaussian quadrature
 η = gamma distribution parameter (minimum molecular
 weight, lbm/lbm mole)
 ω = acentric factor

Acknowledgements

The authors would like to thank Kameshwar Singh for his many contributions to this work, ADNOC and QP for their advices and assistance.

References

1. Fevang, Ø. and Whitson, C.H.: "Accurate In-Situ Compositions in Petroleum Reservoirs," paper SPE 28829 presented at the 1994 European Petroleum Conference, London, 25-27 October.
2. Whitson, C.H., Andersen, T.F., and Søreide, I.: "C₇₊ characterization of Related Equilibrium Fluids Using the Gamma Distribution," *C₇₊ Fraction Characterization*, L.G. Chorn and G.A. Mansoori (eds.), Advances in Thermodynamics, "Taylor & Francis, New York City (1989) 1, 35-56.
3. Whitson, C.H.: "Characterizing Hydrocarbon Plus Fractions," *SPEJ* (August 1983) 683; *Trans.*, AIME, **275**.
4. Whitson, C.H.: "Effect of C₇₊ Properties on Equation-of-State Predictions," paper SPE 11200 presented at the 1982 SPE Annual Technical Conference and Exhibition, New Orleans, 26-29 September.
5. Whitson, C.H.: "Effect of C₇₊ Properties on Equation-of-State Predictions," *SPEJ* (December 1984) 685; *Trans.*, AIME, **277**.
6. Søreide, I.: "Improved Phase behavior Predictions of Petroleum Reservoir Fluids From a Cubic Equation of State." Dr.Ing. dissertation, Norwegian Inst. Of Technology, Trondheim, Norway (1989).
7. Twu, C.H.: "An Internally Consistent Correlation for Predicting the Critical Properties and Molecular Weight of Petroleum and Coal-Tar Liquids," *Fluid Phase Equilibria* (1984) No. 16, 137.
8. Lee, B.I. and Kesler, M.G.: "A Generalized Thermodynamic Correlation Based on Three-Parameter Corresponding State," *AIChE J.* (1975) **21**, 510.
9. Kesler, M.G. and Lee, B.I.: "Improve Prediction of Enthalpy of Fractions," *Hydro. Proc.* (March 1976) **55**, 153.
10. Chueh, P.L. and Prausnitz, J.M.: "Calculation of High-Pressure Vapor-Liquid Equilibria," *Ind. Eng. Chem.* (1968) **60**, No. 13.
11. Firoozabadi, A. *et al.*: "Surface Tension of Reservoir Cruude-Oil/Gas Systems Recognizing the Asphalt in the Heavy Fraction," *SPE* (February 1988) 265.
12. Peneloux, A., Rauzy, E., and Freze, R.: "A Consistent Correlation for Redlich-Kwong-Soave Volumes," *Fluid Phase Equilibria* (1982) **8**, 7.
13. Jhaveri, B.S. and Youngren, G.K.: "Three-Parameter Modification of the Peng-Robinson Equation of State To Improve Volumetric Predictions," *SPE* (August 1988) 1033.
14. Peng, D.Y. and Robinson, D.B.: "A New-Constant Equation of State," *Ind. & Eng. Chem.* (1976) **15**, No. 1, 59.
15. Lohrenz, J., Bray, B.G., and Clark, C.R.: "Calculating Viscosities of Reservoir Fluids From Their Compositions," *JPT* (October 1964) 1171; *Trans.*, AIME, **231**.
16. Fevang, Ø., Singh, K. and Whitson, C.H.: "Guidelines for Choosing Compositional and Black-Oil Models for Volatile Oil and Gas-Condensate Reservoirs," paper SPE 63087 presented at the 2000 SPE Annual Technical Conference and Exhibition, Dallas, 1-4 October.

Table 1 Initial EOS parameters

Component	Molecular Weight M_i	Specific Gravity γ_l	Boiling Point T_{bi}	Critical Temperature T_{ci}	Critical Volume v_{ci}	Critical Pressure p_{ci}	Acentric Factor ω_i
N2	28.01300	0.47000	139.2700	227.27000	1.44270	493.00000	0.04500
CO2	44.01000	0.50720	350.3700	547.57000	1.50510	1070.60000	0.23100
H2S	34.07600	0.50000	383.0700	672.37000	1.56410	1306.00000	0.10000
C1	16.04300	0.33000	200.9800	343.04000	1.58990	667.80000	0.01150
C2	30.07000	0.45000	332.1900	549.76000	2.36950	707.80000	0.09080
C3	44.09700	0.50770	416.0000	665.68000	3.24990	616.30000	0.14540
iC4	58.12400	0.56310	470.5700	734.65000	4.20820	529.10000	0.17560
nC4	58.12400	0.58440	490.7700	765.32000	4.08030	550.70000	0.19280
iC5	72.15100	0.62470	541.7900	828.77000	4.89910	490.40000	0.22730
nC5	72.15100	0.63100	556.5900	845.37000	4.87020	488.60000	0.25100
C6	86.17800	0.66400	615.3900	913.37000	5.92900	436.90000	0.29570
C7-1	98.54849	0.74796	674.4849	1008.25891	6.36557	450.06335	0.280235
C7-2	135.84324	0.79613	795.5029	1140.94704	8.40055	370.25151	0.382200
C7-3	206.64883	0.84473	974.1083	1316.43302	12.28557	274.65746	0.567094
C7-4	319.82579	0.88932	1175.2330	1497.26480	17.68981	199.48636	0.817612
C7-5	500.00000	0.93290	1383.6195	1677.40288	23.74459	148.94966	1.093874

Component	Omega A Ω_a	Omega B Ω_b	Shift Parameter s_i	Parachor P_i	Methane BIP's $k(i,j)$	H2S BIP's $k(i,j)$
N ₂	0.457236	0.077796	-0.19300	41.00000	0.02500	0.00000
CO ₂	0.457236	0.077796	-0.08200	70.00000	0.10500	0.00000
H ₂ S	0.457236	0.077796	-0.12900	41.00000	0.07000	-
C ₁	0.457236	0.077796	-0.15900	77.00000	-	0.07000
C ₂	0.457236	0.077796	-0.11300	108.00000	0.00000	0.08500
C ₃	0.457236	0.077796	-0.08600	150.30000	0.00000	0.08000
iC ₄	0.457236	0.077796	-0.08400	181.50000	0.00000	0.07500
nC ₄	0.457236	0.077796	-0.06700	189.90000	0.00000	0.07500
iC ₅	0.457236	0.077796	-0.06100	225.00000	0.00000	0.07000
nC ₅	0.457236	0.077796	-0.03900	231.50000	0.00000	0.05500
C ₆	0.457236	0.077796	-0.00800	271.00000	0.00000	0.05000
C ₇₋₁	0.457236	0.077796	0.025862	308.34565	0.03061	0.05000
C ₇₋₂	0.457236	0.077796	0.049412	409.57621	0.04245	0.05000
C ₇₋₃	0.457236	0.077796	0.094901	584.92748	0.05965	0.05000
C ₇₋₄	0.457236	0.077796	0.129727	819.40253	0.07856	0.05000
C ₇₋₅	0.457236	0.077796	0.120350	1076.40000	0.09778	0.05000

Table 2 Tuned EOS parameters

Component	Molecular Weight M_i	Specific Gravity γ_i	Boiling Point T_{bi}	Critical Temperature T_{ci}	Critical Volume V_{ci}	Critical Pressure P_{ci}	Acentric Factor ω_i
N ₂	28.01300	0.47000	139.2700	227.27000	1.44270	493.00000	0.045000
CO ₂	44.01000	0.50720	350.3700	547.57000	1.50510	1070.60000	0.231000
H ₂ S	34.07600	0.50000	383.0700	672.37000	1.56410	1306.00000	0.100000
C ₁	16.04300	0.33000	200.9800	343.04000	1.58990	667.80000	0.011500
C ₂	30.07000	0.45000	332.1900	549.76000	2.36950	707.80000	0.090800
C ₃	44.09700	0.50770	416.0000	665.68000	3.24990	616.30000	0.145400
iC ₄	58.12400	0.56310	470.5700	734.65000	4.20820	529.10000	0.175600
nC ₄	58.12400	0.58440	490.7700	765.32000	4.08030	550.70000	0.192800
iC ₅	72.15100	0.62470	541.7900	828.77000	4.89910	490.40000	0.227300
nC ₅	72.15100	0.63100	556.5900	845.37000	4.87020	488.60000	0.251000
C ₆	86.17800	0.66400	615.3900	913.37000	5.92900	436.90000	0.295700
C ₇₋₁	98.54849	0.74796	674.4849	1024.77540	7.82676	440.31489	0.319036
C ₇₋₂	135.84324	0.79613	795.5029	1159.63712	10.07839	362.23179	0.442955
C ₇₋₃	206.64883	0.84473	974.1083	1423.60963	14.04390	277.22913	0.645622
C ₇₋₄	319.82579	0.88932	1175.2330	1434.73033	18.62099	200.81341	0.912791
C ₇₋₅	500.00000	0.93290	1383.6195	1672.08484	21.57420	145.46327	1.191996

Component	Omega A Ω_a	Omega B Ω_b	Shift Parameter s_i	Parachor P_i	Methane BIP's $k(i,j)$	H2S BIP's $k(i,j)$
N ₂	0.457236	0.077796	-0.19300	41.00000	0.02500	0.00000
CO ₂	0.457236	0.077796	-0.08200	70.00000	0.10500	0.00000
H ₂ S	0.457236	0.077796	-0.12900	41.00000	0.07000	-
C ₁	0.457236	0.077796	-0.15900	77.00000	-	0.07000
C ₂	0.457236	0.077796	-0.11300	108.00000	0.00000	0.08500
C ₃	0.457236	0.077796	-0.08600	150.30000	0.00000	0.08000
iC ₄	0.457236	0.077796	-0.08400	181.50000	0.00000	0.07500
nC ₄	0.457236	0.077796	-0.06700	189.90000	0.00000	0.07500
iC ₅	0.457236	0.077796	-0.06100	225.00000	0.00000	0.07000
nC ₅	0.457236	0.077796	-0.03900	231.50000	0.00000	0.05500
C ₆	0.457236	0.077796	-0.00800	271.00000	0.00000	0.05000
C ₇₋₁	0.436248	0.077796	0.06778	308.34565	0.02057	0.16591
C ₇₋₂	0.424900	0.077796	0.09050	409.57621	0.02844	0.16591
C ₇₋₃	0.339813	0.077796	0.17200	584.92748	0.03981	0.16591
C ₇₋₄	0.557905	0.077796	0.07386	819.40253	0.05218	0.16591
C ₇₋₅	0.435206	0.077796	0.13886	1076.40000	0.06459	0.16591

Table 3 Comparison of ECM Gas Compositions

Component	Observed	Initial EOS	Final EOS
N ₂	0.0068	0.0069	0.0059
CO ₂	0.0547	0.0555	0.0536
H ₂ S	0.1139	0.1142	0.1250
C ₁	0.5558	0.6083	0.5518
C ₂	0.0743	0.0715	0.0723
C ₃	0.0452	0.0411	0.0441
iC ₄	0.0094	0.0082	0.0092
nC ₄	0.0217	0.0187	0.0213
iC ₅	0.0094	0.0080	0.0095
nC ₅	0.0108	0.0091	0.0109
C ₆	0.0142	0.0117	0.0147
C ₇₋₁	0.0255	0.0069	0.0094
C ₇₋₂	0.0330	0.0226	0.0352
C ₇₋₃	0.0169	0.0143	0.0315
C ₇₋₄	0.0067	0.0027	0.0050
C ₇₋₅	0.0017	0.0001	0.0005

Table 4 Comparison of ECM Oil Compositions

Component	Observed	Initial EOS	Final EOS
N ₂	0.0045	0.0049	0.0045
CO ₂	0.0488	0.0507	0.0493
H ₂ S	0.1202	0.1225	0.1174
C ₁	0.4682	0.4939	0.4699
C ₂	0.0706	0.0719	0.0714
C ₃	0.0462	0.0464	0.0470
iC ₄	0.0101	0.0100	0.0102
nC ₄	0.0239	0.0236	0.0245
iC ₅	0.0115	0.0109	0.0114
nC ₅	0.0135	0.0127	0.0134
C ₆	0.0189	0.0178	0.0190
C ₇₋₁	0.0389	0.0124	0.0138
C ₇₋₂	0.0588	0.0518	0.0597
C ₇₋₃	0.0371	0.0504	0.0587
C ₇₋₄	0.0209	0.0181	0.0267
C ₇₋₅	0.0078	0.0020	0.0030

Table 5 Pseudoized EOS parameters

Component	Molecular Weight M_i	Specific Gravity γ_i	Boiling Point T_{bi}	Critical Temperature T_{ci}	Critical Volume V_{ci}	Critical Pressure P_{ci}
C ₁ N ₂	16.19542	0.33218	199.6208	340.49020	1.58666	663.95010
C ₂ CO ₂	35.93076	0.47775	341.5520	548.63220	1.92437	894.62860
H ₂ S	34.07600	0.50000	383.0700	672.37000	1.56410	1306.00000
C ₃ C ₄	50.02873	0.53992	449.7788	710.14530	3.67660	580.90920
C ₅ C ₆	78.27134	0.64465	580.8787	873.5969	4.31320	464.24470
C _{7-1&2}	128.9243	0.78892	778.3409	1140.51100	10.89949	373.30280
C ₇₋₃	206.64883	0.84473	974.1083	1423.60963	14.04390	277.22913
C ₇₋₄	319.82579	0.88932	1175.2330	1434.73033	18.62099	200.81341
C ₇₋₅	500.00000	0.93290	1383.6195	1672.08484	21.57420	145.46327

Component	Acentric Factor ω_i	Omega A Ω_a	Omega B Ω_b	Shift Parameter s_i	Parachor P_i
C ₁ N ₂	0.01224	0.457236	0.077796	-0.15939	76.54160
C ₂ CO ₂	0.16300	0.457236	0.077796	-0.10298	92.02375
H ₂ S	0.10000	0.457236	0.077796	-0.12900	41.00000
C ₃ C ₄	0.16617	0.457236	0.077796	-0.07926	165.98790
C ₅ C ₆	0.26613	0.457236	0.077796	-0.02954	246.84860
C _{7-1&2}	0.42538	0.457236	0.077796	0.08713	390.79590
C ₇₋₃	0.64562	0.339813	0.077796	0.17200	584.92748
C ₇₋₄	0.91279	0.557905	0.077796	0.07386	819.40253
C ₇₋₅	1.19200	0.435206	0.077796	0.13886	1076.40000

Component	C ₁ N ₂	C ₂ CO ₂	H ₂ S	C ₃ C ₄	C ₅ C ₆	C _{7-1&2}	C ₇₋₃	C ₇₋₄
C ₂ CO ₂	0.05299							
H ₂ S	0.06846	0.04123						
C ₃ C ₄	0.00204	0.06222	0.07754					
C ₅ C ₆	0.00236	0.05922	0.05661	0.00000				
C _{7-1&2}	0.03787	0.05922	0.16591	0.00000	0.00000			
C ₇₋₃	0.04136	0.05922	0.16591	0.00000	0.00000	0.00000		
C ₇₋₄	0.05345	0.05922	0.16591	0.00000	0.00000	0.00000	0.00000	
C ₇₋₅	0.06559	0.05922	0.16591	0.00000	0.00000	0.00000	0.00000	0.00000

Table 6 Comparison of Calculated GOC Gas Compositions

Component	Old EOS	Final EOS
N ₂	0.0090	0.0081
CO ₂	0.0605	0.0585
H ₂ S	0.0850	0.1033
C ₁	0.6204	0.5602
C ₂	0.0755	0.0749
C ₃	0.0446	0.0423
iC ₄	0.0099	0.0088
nC ₄	0.0211	0.0200
iC ₅	0.0077	0.0115
nC ₅	0.0077	0.0106
C ₆	0.0132	0.0159
C ₇₊	0.0454	0.0860

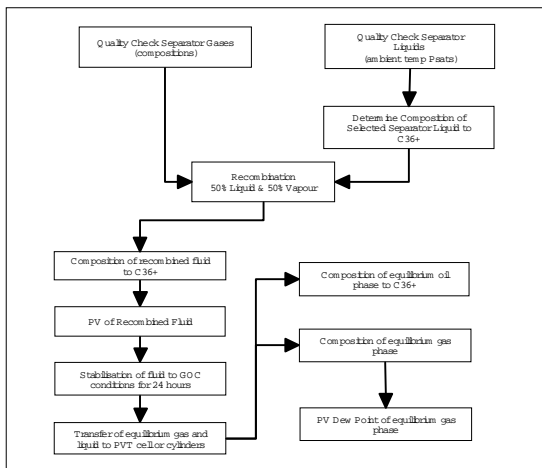


Fig. 1 ECM Experiment Procedure

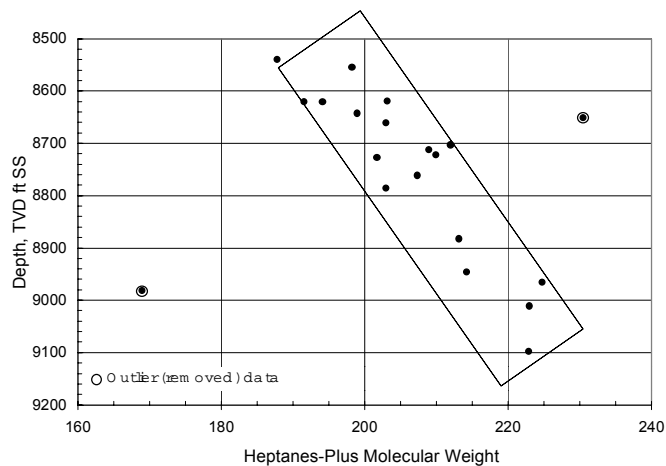


Fig. 4 Measured C₇₊ molecular weight versus Depth

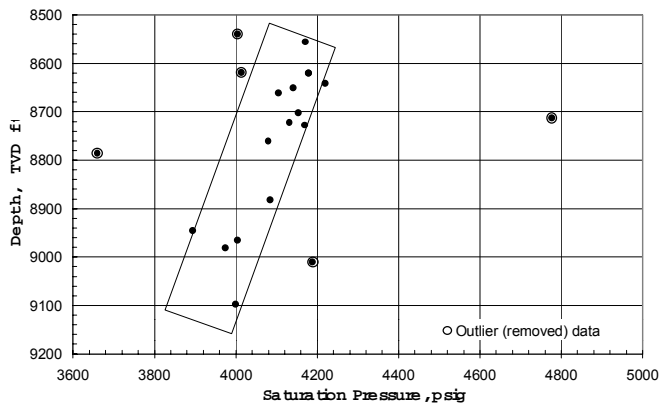


Fig. 2 Measured Saturation Pressure versus Depth

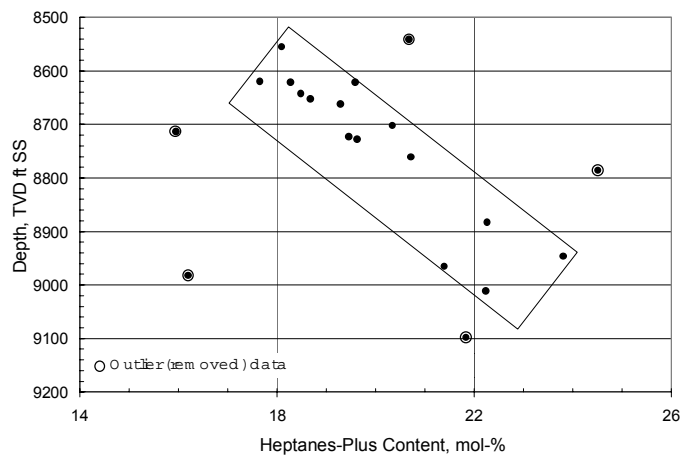


Fig. 5 Measured C₇₊ amount versus Depth

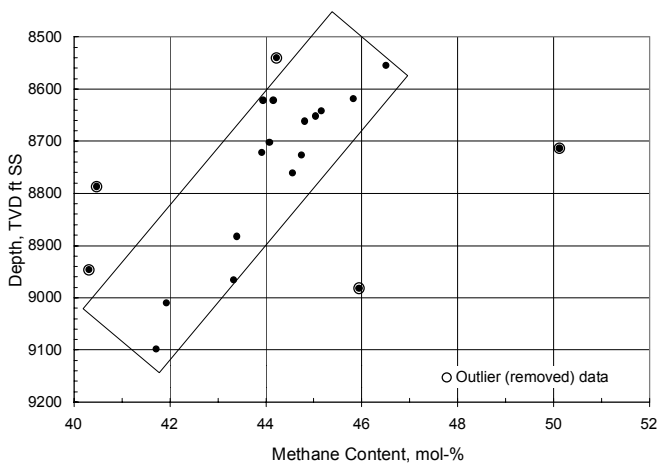


Fig. 3 Measured Methane Content versus Depth

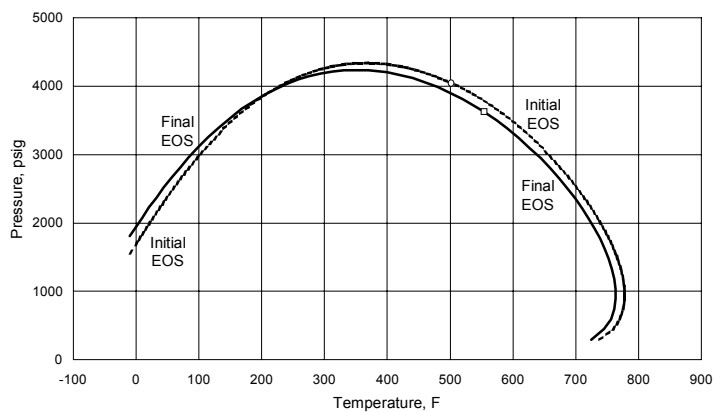


Fig. 6 Phase Plot of Initial and Final EOS

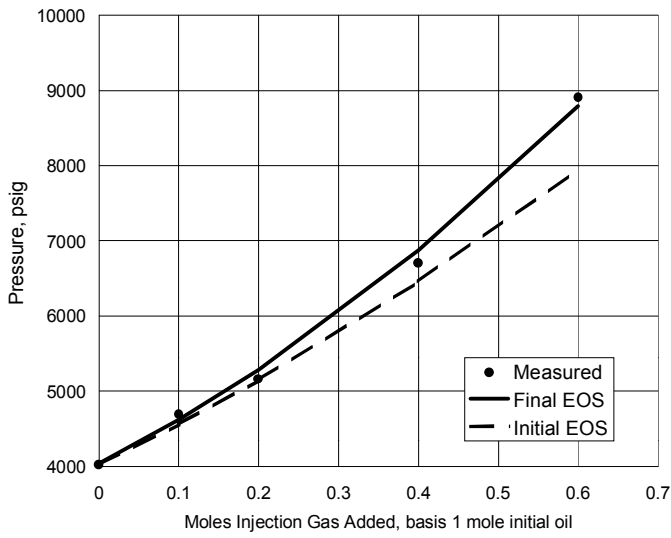


Fig. 7 Measured and Calculated Saturation Pressure in MCV Well A

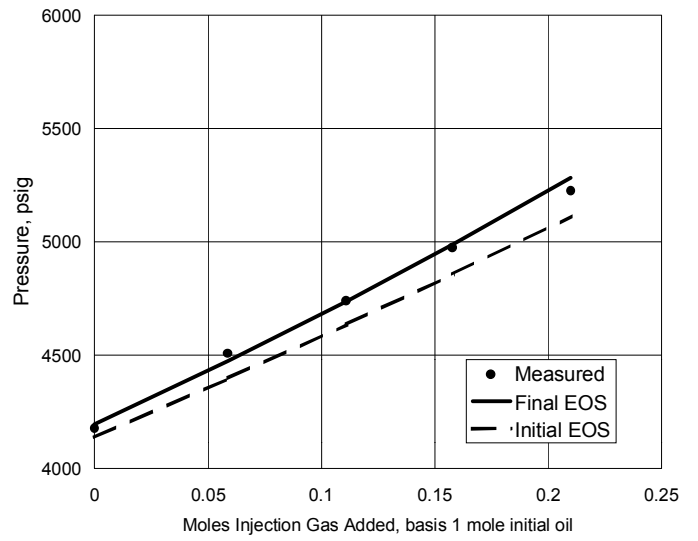


Fig. 9 Measured and Calculated Saturation Pressure in MCV Well C

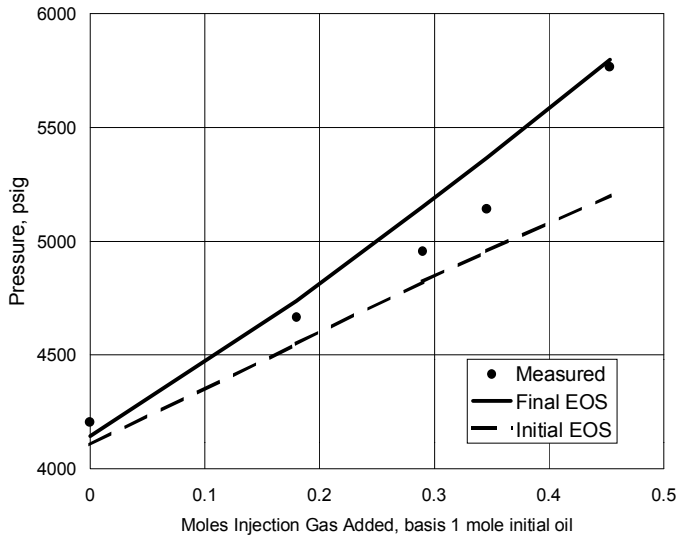


Fig. 8 Measured and Calculated Saturation Pressure in MCV Well B

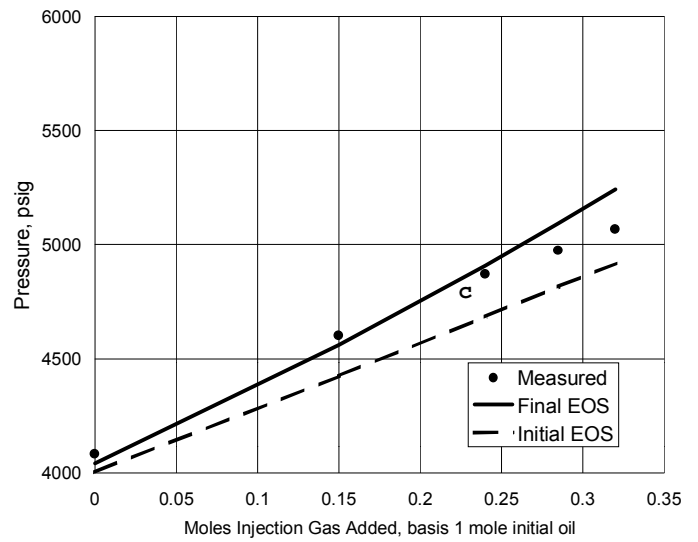


Fig. 10 Measured and Calculated Saturation Pressure in MCV Well D

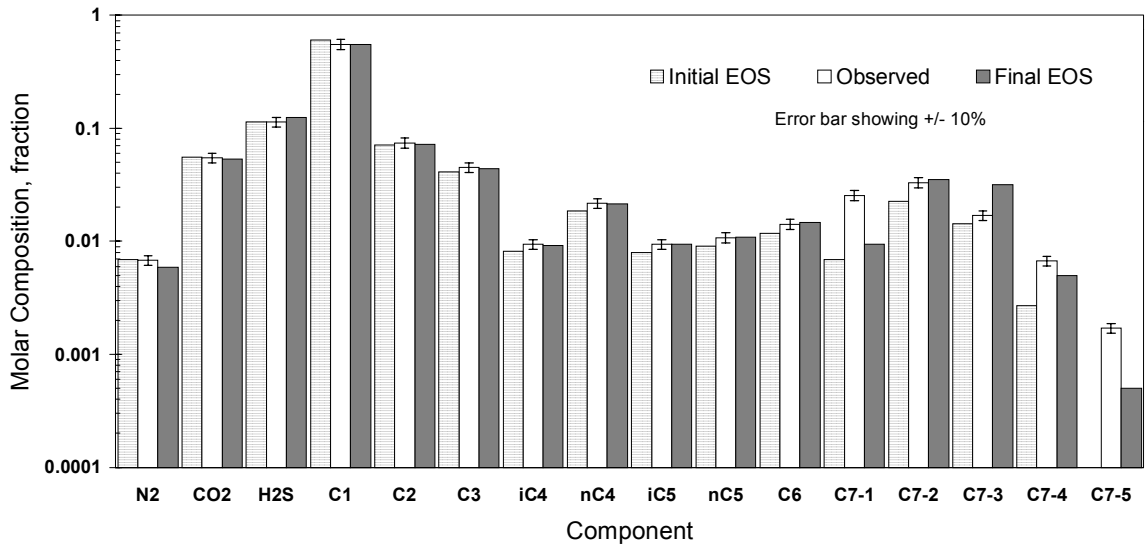


Fig. 11 Measured and Calculated (Initial and Final EOS) ECM Gas Composition

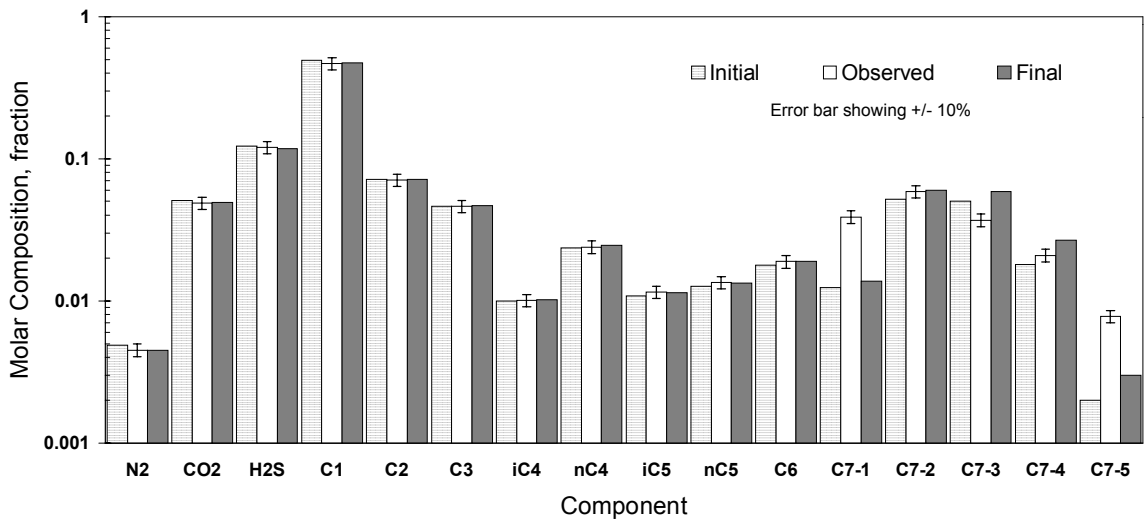


Fig. 12 Measured and Calculated (Initial and Final EOS) ECM Oil Composition

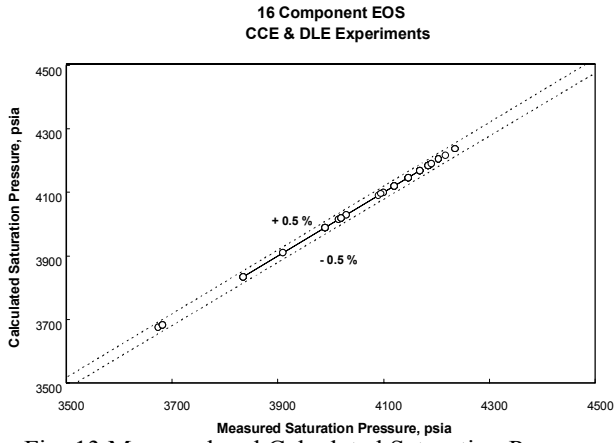


Fig. 13 Measured and Calculated Saturation Pressure

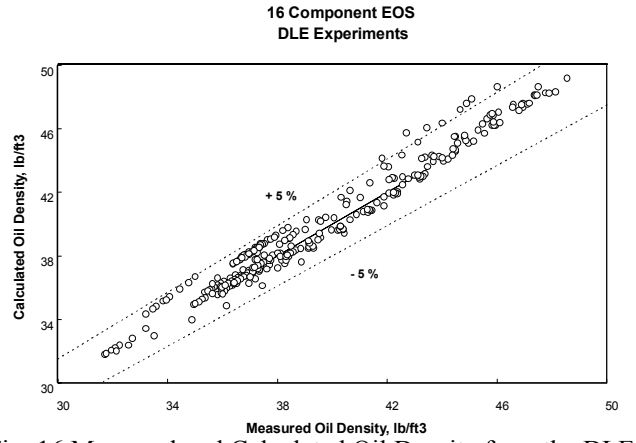


Fig. 16 Measured and Calculated Oil Density from the DLE

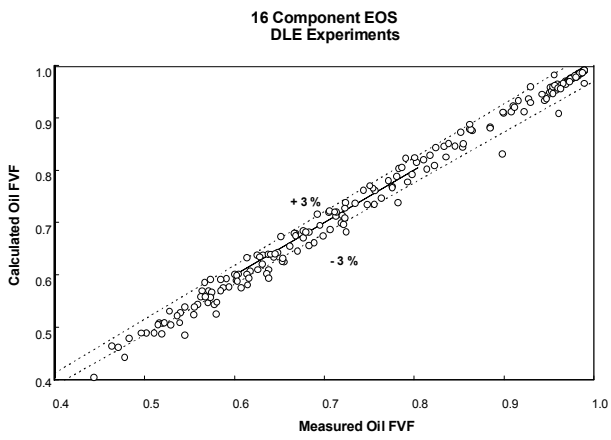


Fig. 14 Measured and Calculated Oil FVF relative to Oil FVF at the Saturation Pressure

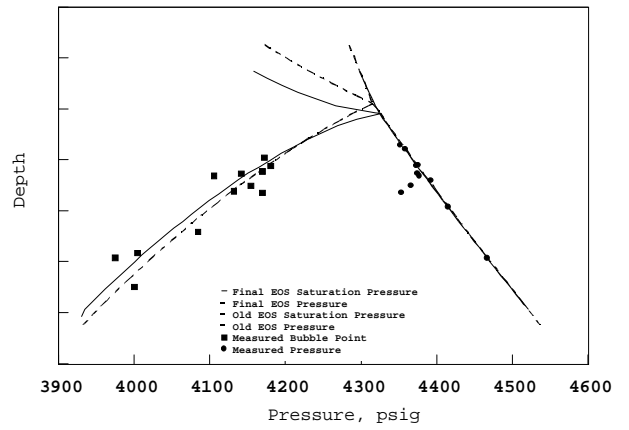


Fig. 17 Gradient Calculation Comparison of Old and New EOS

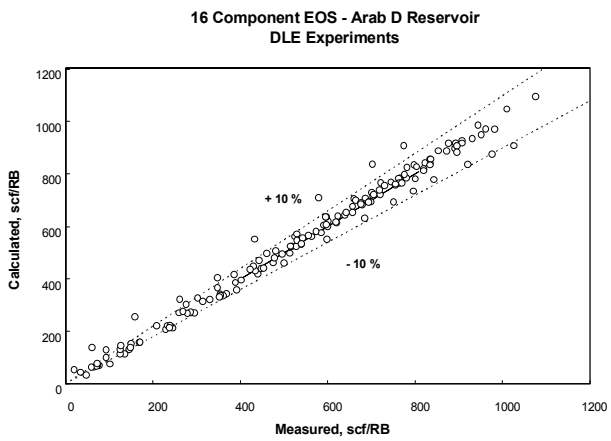


Fig. 15 Measured and Calculated Released Gas from the DLE

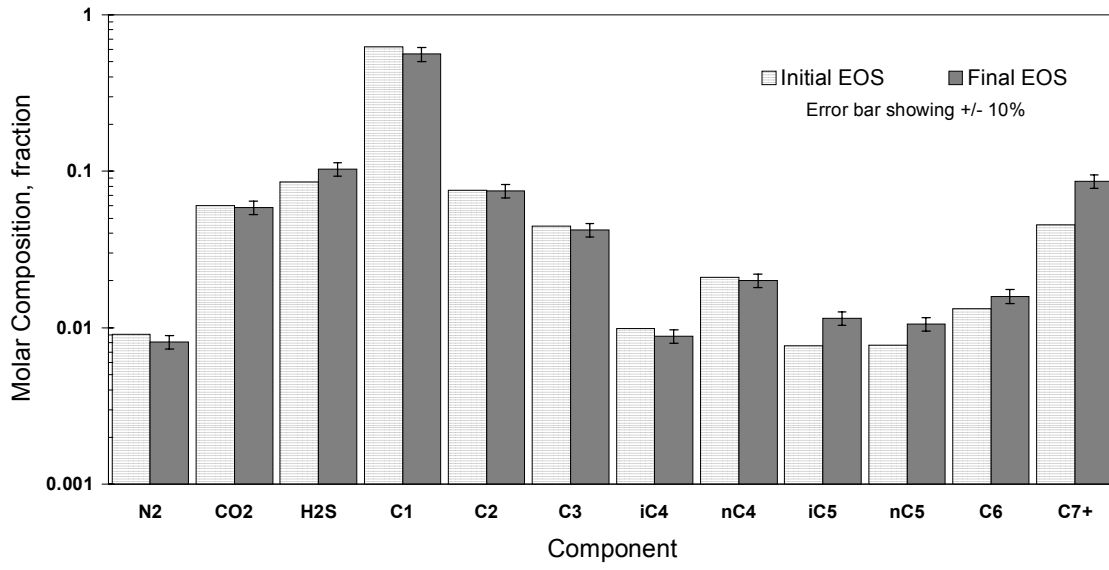


Fig. 18 GOC Gas Composition of Old and New EOS